arXiv:1412.3132v2 [hep-ph] 20 Dec 2014

Single- and central-diffractive production of open charm and bottom mesons at the LHC: theoretical predictions and experimental capabilities

Marta Łuszczak*

University of Rzeszów, PL-35-959 Rzeszów, Poland

Rafał Maciuła† and Antoni Szczurek‡§

Institute of Nuclear Physics PAN, PL-31-342 Cracow, Poland

(Dated: December 23, 2014)

Abstract

We discuss diffractive production of open charm and bottom mesons at the LHC. The differential cross sections for single- and central-diffractive mechanisms for $c\bar{c}$ and $b\bar{b}$ pair production are calculated in the framework of the Ingelman-Schlein model corrected for absorption effects. In this approach one assumes that the pomeron has a well defined partonic structure, and that the hard process takes place in a pomeron-proton or proton-pomeron (single diffraction) or pomeron-pomeron (central diffraction) processes. Here, leading-order gluon-gluon fusion and quark-antiquark anihilation partonic subprocesses are taken into consideration, which are calculated within standard collinear approximation. Both pomeron flux factors as well as parton distributions in the pomeron are taken from the H1 Collaboration analysis of diffractive structure function and diffractive dijets at HERA. The extra corrections from subleading reggeon exchanges are explicitly calculated and are also taken into consideration. Several quark-level differential distributions are shown. The hadronization of charm and bottom quarks is taken into account by means of fragmentation function technique. Predictions for single- and central-diffractive production in the case of inclusive D and B mesons, as well as $D\bar{D}$ pairs are presented, including detector acceptance of the ATLAS, CMS and LHCb Collaborations. The experimental aspects of possible standard and dedicated measurements are carefully discussed.

PACS numbers: 13.87.Ce,14.65.Dw

‡ also at University of Rzeszów, PL-35-959 Rzeszów, Poland
*Electronic address: luszczak@univ.rzeszow.pl
†Electronic address: rafal.maciula@ifj.edu.pl
§Electronic address: antoni.szczurek@ifj.edu.pl

I. INTRODUCTION

Diffractive processes were intensively studied at HERA in γp and ep collisions for more than a decade. On theoretical side, somewhat enigmatically, these are processes with exchange of pomeron or processes with the QCD amplitude without net color exchange. In such processes pomeron must be treated rather technically, depending on the formulation of the approach. Experimentally such processes are defined by special requirement(s) on the final state. The most popular is a requirement of rapidity gap starting from the final proton(s) on one (single-diffrative process) or both (central-diffractive process) sides. The size of the gap is essentially experimental observable but it is not easy to calculate theoretically. Several processes with different final states were studied at HERA, such as dijet, charm production, etc. The H1 Collaboration has found a set of so-called diffractive parton distributions in the proton inspired by the Ingelman-Schlein model [1]. In this fit both pomeron and reggeon contributions were included. We wish to emphasize that there is no common consensus as far as a model of diffractive production is considered. However, these open problems go beyond the scope of the present paper and will be not discussed here.

One can gain a better understanding of the mechanism of the diffractive production by going from photon-proton to proton-proton or proton-antiproton scattering. There, however, some new elements related to nonperturbative interaction between protons show up, such as absorption effects. So far only some selected diffractive processes were discussed in the literature such as diffractive production of dijets [2], production of W [3] and Z [4] bosons, production of W^+W^- pairs [5] or production of $c\bar{c}$ [6]. The latter was done there only for illustration of the general situation at the parton level. The cross section for diffractive processes are in general rather small (e.g. the single-diffractive processes are of the order of a few percent compared to inclusive cross sections). In order to measure rapidity gap(s) the luminosity cannot be big to avoid so-called pile-ups [7]. All this causes that for some interesting processes, as for instance W or Z^0 production, the statistics is rather poor and the cross section is difficult to measure. Since the cross section for inclusive production of charm is very large at the LHC [8], one could expect that also single- and central- diffractive charm production could be measured with relatively good precision. This is therefore a process one could use for testing theoretical models. The same shall be true for diffractive bottom production.

It is the aim of this paper to present predictions including our knowledge about diffractive parton distributions from HERA and taking into account absorption effects, specific for proton-proton collisions. We shall include both pomeron and reggeon contributions. In addition, we shall include hadronization of c or b quarks/antiquarks to open charmed and bottom mesons, respectively. Finally we shall present our predictions for experiments at the LHC. We hope that our predictions will be verified at the LHC in a near future.

II. THEORETICAL FRAMEWORK

A. A sketch of formalism

The mechanisms of the diffractive production of heavy quarks ($c\bar{c}$, $b\bar{b}$) discussed here are shown in Figs. 1 and 2. Both, leading-order (LO) gg-fusion and $q\bar{q}$-anihilation partonic subprocesses are taken into account in the calculations.

In the following we apply the Ingelman-Schlein approach [1]. In this approach one assumes

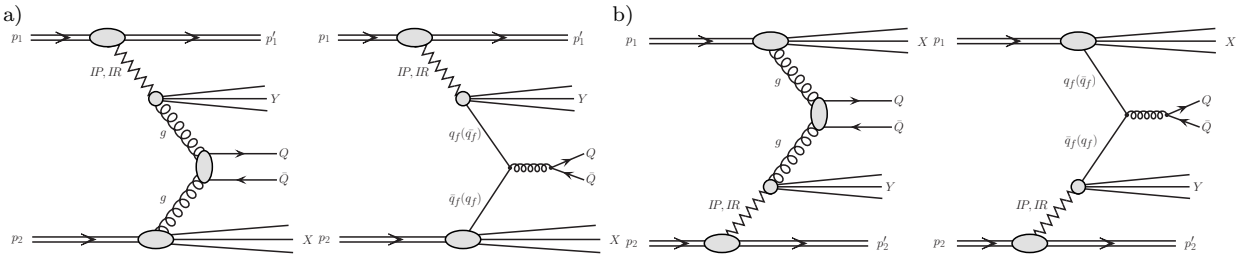

FIG. 1: The mechanisms of single-diffractive production of heavy quarks.

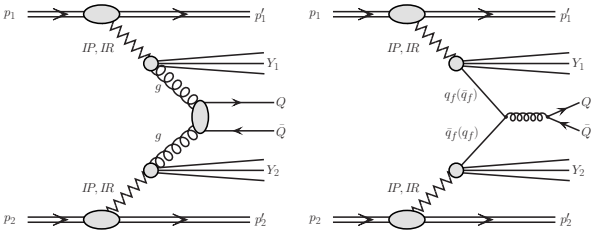

FIG. 2: The mechanisms of central-diffractive production of heavy quarks.

that the pomeron has a well defined partonic structure, and that the hard process takes place in a pomeron–proton or proton–pomeron (single diffraction) or pomeron–pomeron (central diffraction) processes. In this approach corresponding differential cross sections can be written as

$$\frac{d\sigma_{SD^{(1)}}}{dy_1 dy_2 dp_t^2} = \frac{1}{16\pi^2 \hat{s}^2} \times \Big[|\mathcal{M}_{gg\to Q\bar{Q}}|^2 \cdot x_1 g^D(x_1,\mu^2) x_2 g(x_2,\mu^2) + |\mathcal{M}_{q\bar{q}\to Q\bar{Q}}|^2 \cdot \Big(x_1 q^D(x_1,\mu^2) x_2 \bar{q}(x_2,\mu^2) + x_1 \bar{q}^D(x_1,\mu^2) x_2 q(x_2,\mu^2) \Big) \Big] , \quad (2.1)$$

$$\frac{d\sigma_{SD^{(2)}}}{dy_1 dy_2 dp_t^2} = \frac{1}{16\pi^2 \hat{s}^2} \times \Big[|\mathcal{M}_{gg\to Q\bar{Q}}|^2 \cdot x_1 g(x_1,\mu^2) x_2 g^D(x_2,\mu^2) + |\mathcal{M}_{q\bar{q}\to Q\bar{Q}}|^2 \cdot \Big(x_1 q(x_1,\mu^2) x_2 \bar{q}^D(x_2,\mu^2) + x_1 \bar{q}(x_1,\mu^2) x_2 q^D(x_2,\mu^2) \Big) \Big] , \quad (2.2)$$

$$\frac{d\sigma_{CD}}{dy_1 dy_2 dp_t^2} = \frac{1}{16\pi^2 \hat{s}^2} \times \Big[|\mathcal{M}_{gg\to Q\bar{Q}}|^2 \cdot x_1 g^D(x_1,\mu^2) x_2 g^D(x_2,\mu^2) + |\mathcal{M}_{q\bar{q}\to Q\bar{Q}}|^2 \cdot \Big(x_1 q^D(x_1,\mu^2) x_2 \bar{q}^D(x_2,\mu^2) + x_1 \bar{q}^D(x_1,\mu^2)\, x_2 q^D(x_2,\mu^2) \Big) \Big] , \quad (2.3)$$

for single-diffractive (SD) and central-diffractive (CD) production, respectively.

The diffractive distribution function (diffractive PDF) can be obtained by a convolution of the flux of pomerons $f_{I\!P}(x_{I\!P})$ in the proton and the parton distribution in the pomeron, e.g. $g_{I\!P}(\beta,\mu^2)$ for gluons:

$$g^D(x,\mu^2) = \int dx_{I\!P}\, d\beta\, \delta(x - x_{I\!P}\beta) g_{I\!P}(\beta,\mu^2)\, f_{I\!P}(x_{I\!P}) = \int_x^1 \frac{dx_{I\!P}}{x_{I\!P}}\, f_{I\!P}(x_{I\!P}) g_{I\!P}(\frac{x}{x_{I\!P}},\mu^2) . \quad (2.4)$$

The flux of pomerons $f_{I\!P}(x_{I\!P})$ enters in the form integrated over four–momentum transfer

$$f_{I\!P}(x_{I\!P}) = \int_{t_{min}}^{t_{max}} dt\, f(x_{I\!P}, t)\,, \tag{2.5}$$

with t_{min}, t_{max} being kinematic boundaries.

Both pomeron flux factors $f_{I\!P}(x_{I\!P}, t)$ as well as parton distributions in the pomeron were taken from the H1 Collaboration analysis of diffractive structure function and diffractive dijets at HERA [9]. In the following calculation standard collinear MSTW08LO parton distributions are used [10]. The renormalization scale in α_s and factorization scale for the diffractive PDFs are taken to be equal to heavy quark transverse mass $\mu = m_t$ as a default and $\mu = \hat{s}$ for illustration of related uncertainty. The heavy quark mass in the calculation is set to 1.5 and 4.75 GeV for charm and bottom, respectively.

B. Results for diffractive $Q\bar{Q}$ pair production

Let us start presentation of our results for diffraction mechanisms. In the present analysis we consider both pomeron and subleading reggeon contributions. In the H1 Collaboration analysis the pion structure function was used for the subleading reggeons and the corresponding flux was fitted to the diffractive DIS data. The corresponding diffractive parton distributions are obtained by replacing the pomeron flux by the reggeon flux and the parton distributions in the pomeron by their counterparts in subleading reggeon [9].

In Fig. 3 we show the transverse momentum distribution of c quarks (antiquarks) and b quarks (antiquarks) for single-diffractive production at $\sqrt{s} = 14$ TeV. Contributions of the pomeron-gluon (and gluon-pomeron), the pomeron-quark(antiquark) (and quark(antiquark)-pomeron) and the reggeon-gluon (and gluon-reggeon), the reggeon-quark(antiquark) (and quark(antiquark)-reggeon) mechanisms are shown separately. Components of the pomeron-gluon (and gluon-pomeron) are almost two orders of magnitude larger than the pomeron-quark(antiquark) and quark(antiquark)-pomeron. The estimated reggeon contribution is of similar size as the leading pomeron contribution, but still slightly smaller.

The calculation done assumes Regge factorization, which is known to be violated in hadron-hadron collisions. It is known that soft interactions lead to an extra production of particles which fill in the rapidity gaps related to pomeron exchange.

Different models of absorption corrections (one-, two- or three-channel approaches) for diffractive processes were presented in the literature. The absorption effects for the diffractive processes were calculated e.g. in [4, 11, 12]. The different models give slightly different predictions. Usually an average value of the gap survival probability $< |S_G|^2 >$ is calculated first and then the cross sections for different processes is multiplied by this value. We shall follow this somewhat simplified approach also here. Numerical values of the gap survival probability can be found in [4, 11, 12]. The survival probability depends on the collision energy. It is sometimes parametrized as:

$$< S_G^2 > (\sqrt{s}) = \frac{a}{b + \ln(\sqrt{s})}\,. \tag{2.6}$$

The multiplicative factors are approximately $S_G = 0.05$ for single-diffractive production and $S_G = 0.02$ for central-diffractive one for the nominal LHC energy ($\sqrt{s} = 14$ TeV).

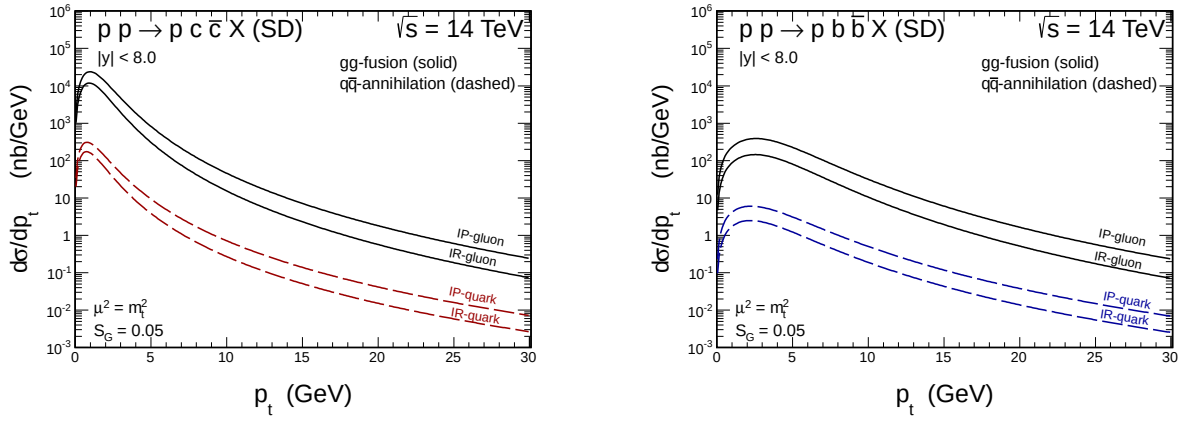

FIG. 3: Transverse momentum distribution of c quarks (antiquarks) (left) and b quarks (antiquarks) (right) for single-diffractive production at $\sqrt{s} = 14$ TeV. Components of the pomeron-gluon (and gluon-pomeron), the pomeron-quark(antiquark) (and quark(antiquark)-pomeron) and the reggeon-gluon (and gluon-reggeon), the reggeon-quark(antiquark) (and quark(antiquark)-reggeon) mechanisms are shown separately.

In Fig. 4 we show the transverse momentum distribution of c quarks (antiquarks) and b quarks (antiquarks) for central-diffractive production at $\sqrt{s} = 14$ TeV. The distributions for central-dffractive component is smaller than that for the single-diffractive distributions by almost two orders of magnitude.

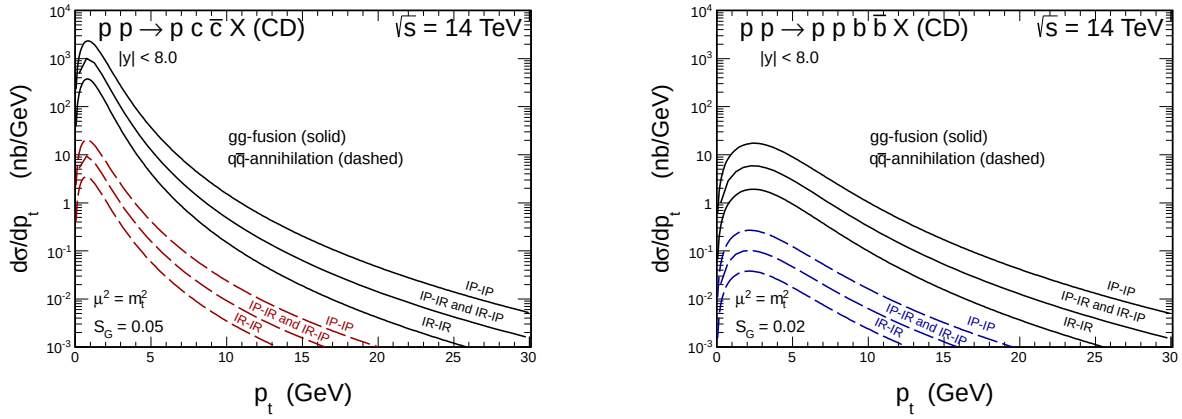

FIG. 4: Transverse momentum distribution of c quarks (antiquarks) (left) and b quarks (antiquarks) (right) for the central-diffractive production at $\sqrt{s} = 14$ TeV. Components of the pomeron-pomeron, reggeon-reggeon, Pomerom-reggeon and reggeon-pomeron mechanisms are shown separately.

In Fig. 5 we show separately contributions for different upper limits for the value of $x_{\mathbb{P}}$ and $x_{\mathbb{R}}$. The shape of these distributions are rather similar. As a default, in the case of pomeron exchange the upper limit in the convolution formula is taken to be 0.1 and for reggeon exchange 0.2. Additionally Fig. 6 shows distribution in pomeron/reggeon longitudinal momentum fraction for c quarks (antiquarks) (left panel) and for b quarks (antiquarks) (right panel) for single-diffractive production. The similar distributions in

$\log_{10} x_{\mathbb{P}}$ and $\log_{10} x_{\mathbb{R}}$ are presented in Fig. 7. In our opinion, the whole Regge formalism does not apply above these limits and therefore unphysical results could be obtained.

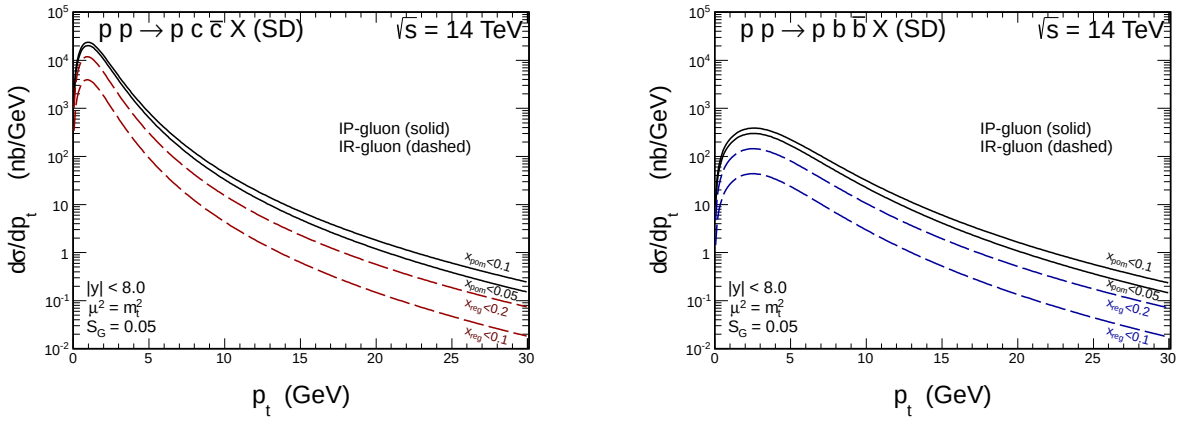

FIG. 5: Transverse momentum distribution of c quarks (antiquarks) (left) and b quarks (antiquarks) (right) for single-diffractive production at $\sqrt{s} = 14$ TeV for different maximal $x_{\mathbb{P}}$ (solid) and $x_{\mathbb{R}}$ (dashed).

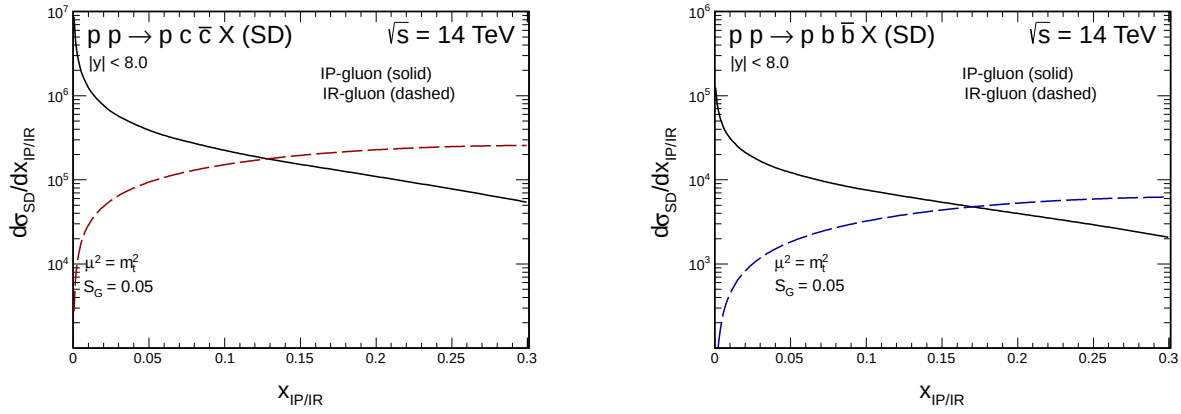

FIG. 6: The distribution in $x_{\mathbb{P}}$ (solid) and $x_{\mathbb{R}}$ (dashed) for $\sqrt{s} = 14$ TeV. The left panel shows distribution in pomeron/reggeon longitudinal momentum fraction for c quarks (antiquarks), the right panel shows similar distributions for b quarks (antiquarks) for single-diffractive production.

For completeness, in Fig. 8 we show separately contributions for different factorization scales: $\mu^2 = m_t^2$ and $\mu^2 = \hat{s}$, which give quite similar distributions in transverse momentum.

Figures 9 and 10 show rapidity distributions for c quarks (antiquarks) (left panels) and b quarks (antiquarks) (right panels) pair production for single- and central-diffractive mechanisms respectively. The rapidity distributions for pomeron-gluon (and gluon-pomeron), pomeron-quark(antiquark) (and quark(antiquark)-pomeron) and reggeon-gluon (and gluon-reggeon), reggeon-quark(antiquark) (and quark(antiquark)-reggeon mechanisms in the single-diffractive case are shifted to forward and backward rapidities, respectively. The distributions for the individual single-diffractive mechanisms have maxima at

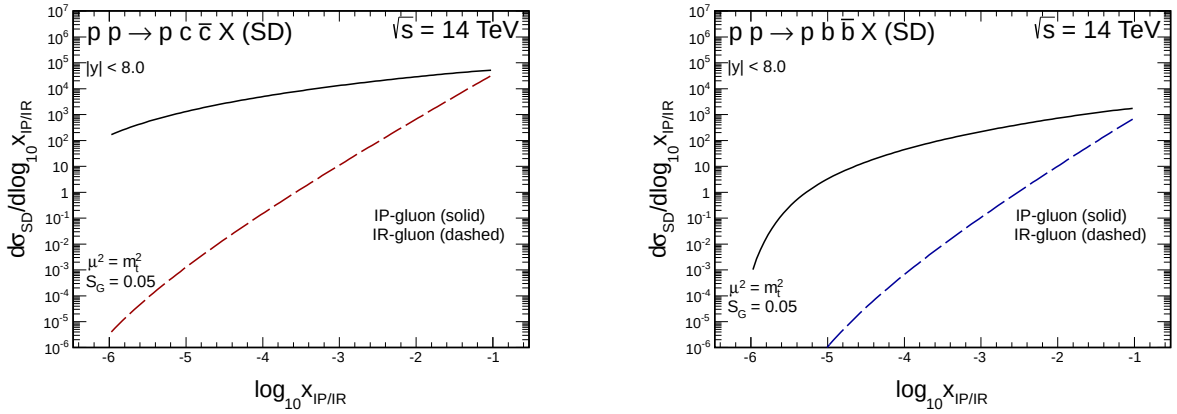

FIG. 7: The distribution in $\log_{10} x_{\mathbb{P}}$ (solid) and $\log_{10} x_{\mathbb{R}}$ (dashed) for $\sqrt{s} = 14$ TeV. The left panel shows distribution for c quarks (antiquarks) and the right panel for b quarks (antiquarks) distribution for single-diffractive production.

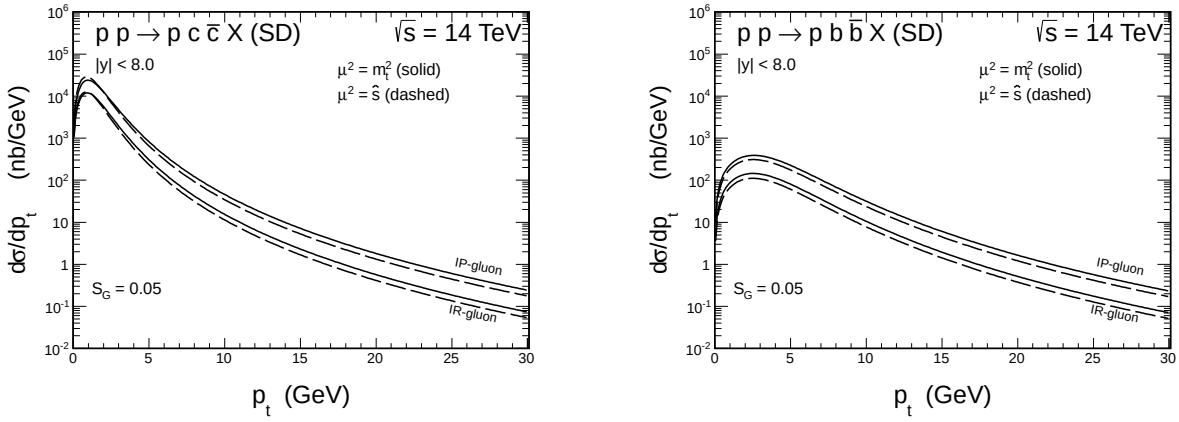

FIG. 8: Transverse momentum distribution of c quarks (antiquarks) (left) and b quarks (antiquarks) (right) for single-diffractive production at $\sqrt{s} = 14$ TeV for factorization scales: $\mu^2 = m_t^2$ (solid) and $\mu^2 = \hat{s}$ (dashed).

large rapidities, while the central-diffractive contribution is concentrated at midrapidities. This is a consequence of limiting integration over $x_{\mathbb{P}}$ in Eq.(2.5) to $0.0 < x_{\mathbb{P}} < 0.1$ and over $x_{\mathbb{R}}$ to $0.0 < x_{\mathbb{R}} < 0.2$.

Finally, In Fig. 11 we show the missing mass distribution for c quarks (antiquarks) (left panel) and for b quarks (antiquarks) (right panel) for single-diffractive production. These both contributions have similar shapes of distributions. Experimentally, measuring the distributions in invariant mass of D and B mesons would be interesting and will be discussed in the next section.

C. Heavy quark hadronization effects

The transition from quarks and gluons to hadrons, called hadronization or parton fragmentation, can be so far approached only through phenomenological models. In principle,

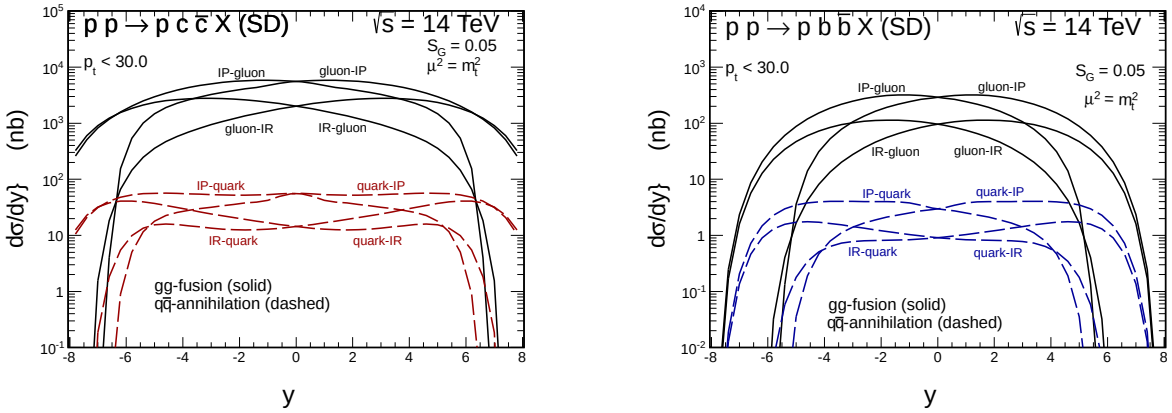

FIG. 9: Rapidity distribution of c quarks (antiquarks) (left) and b quarks (antiquarks) (right) for single-diffractive production at $\sqrt{s} = 14$ TeV. Components of the pomeron-gluon (and gluon-pomeron), the pomeron-quark(antiquark) (and quark(antiquark)-pomeron) and the reggeon-gluon (and gluon-reggeon), the reggeon-quark(antiquark) (and quark(antiquark)-reggeon) mechanisms are shown separately.

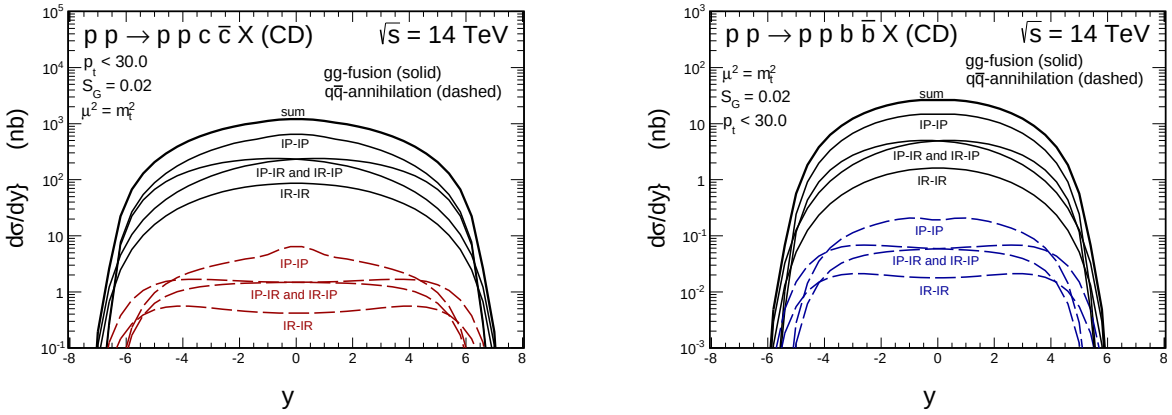

FIG. 10: Rapidity distribution of c quarks (antiquarks) (left) and b quarks (antiquarks) (right) for the central-diffractive production at $\sqrt{s} = 14$ TeV. Components of the pomeron-pomeron, reggeon-reggeon, pomeron-reggeon and reggeon-pomeron mechanisms are shown separately. The sum of all contributions is shown by the thick solid line.

in the case of many-particle final states the Lund string model [13] and the cluster fragmentation model [14] are usually used, providing good description of the hadronization of the parton system as a whole. However, the hadronization of heavy quarks is usually done with the help of fragmentation functions (FFs) extracted from e^+e^- experiments (see e.g. Refs. [8, 15, 16]).

Especially in the case of diffractive production, where one or both protons remain intact, the applicability of the compound hadronization models (implemented in Monte Carlo generators and dedicated to non-diffractive processes) is still an open question. More detailed studies, e.g. of gluonic and quark jet structures in diffractive events, are needed to draw more definite conclusions in this context. In our calculation we follow the fragmentation

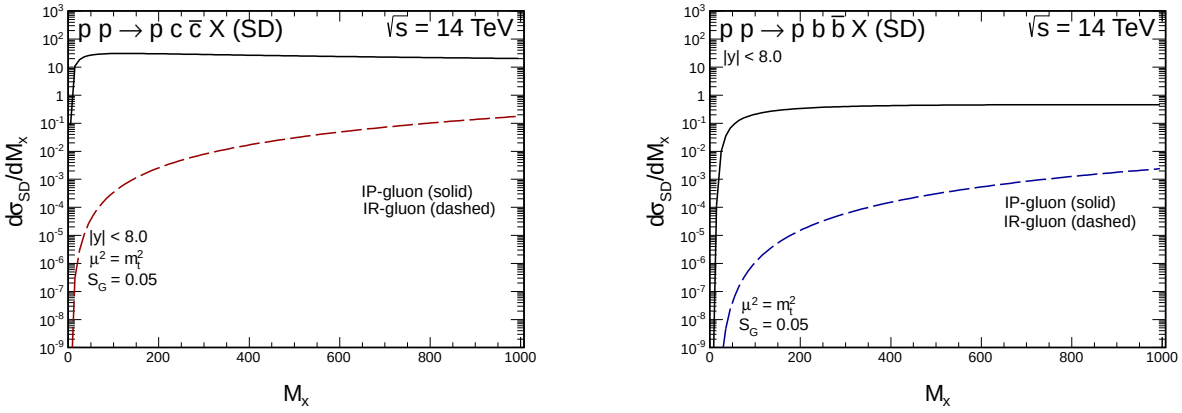

FIG. 11: The missing mass distribution for $\sqrt{s} = 14$ TeV. The left panel shows distribution for c quarks (antiquarks), the right panel b quarks (antiquarks) production for single-diffractive production.

function technique which seems to be sufficient to make first evaluation of corresponding cross sections. This scheme has been recently successfully used for description of inclusive non-diffractive open charm and bottom data at the LHC [8, 16]. In the context of diffractive production studies, the uncertainties coming from the process of parton fragmentation seem to be less important than those related to the parton-level diffractive calculation (e.g. uncertainties of diffractive PDFs or gap survival probability).

According to the fragmentation function formalism, in the following numerical calculations, the differential distributions of open charm and bottom hadrons $h = D, B$, e.g. for single-diffractive production, are obtained through a convolution of differential distributions of heavy quarks/antiquarks and $Q \to h$ fragmentation functions:

$$\frac{d\sigma(pp \to h\bar{h}\, pX)}{dy_h d^2p_{t,h}} \approx \int_0^1 \frac{dz}{z^2} D_{Q\to h}(z) \frac{d\sigma(pp \to Q\overline{Q}\, pX)}{dy_Q d^2p_{t,Q}} \Bigg|_{\substack{y_Q = y_h \\ p_{t,Q} = p_{t,h}/z}} , \tag{2.7}$$

where $p_{t,Q} = \frac{p_{t,h}}{z}$ and z is the fraction of longitudinal momentum of heavy quark Q carried by a hadron h. Technically, in this scheme of fragmentation the rescalling of the transverse momentum is the most important effect. This is because one needs to deal with very steep functions of transverse momenta. Since the rapidity spectra are usually flat, or slowly varying, the approximation assuming that y_Q is unchanged in the fragmentation process, i.e. $y_h = y_Q$, is commonly applied. This approximation is typical for light hadrons, however, is also commonly accepted for heavy quarks, especially in the region of not too small quark p_t's. The fragmentation functions for heavy quarks are peaked at large z (see Fig. 12) so the problematic small-p_t region is suppressed.

In all the following numerical calculations the standard Peterson fragmentation function [17] is applied. The default set of the parameters for these functions is $\varepsilon_c = 0.05$ for charm and $\varepsilon_b = 0.004$ for bottom quarks, respectively. This values were extracted by H1 [18], ALEPH [19] and OPAL [20] analyses. However, in the similar fragmentation scheme applied in the FONLL framework for hadroproduction of heavy flavours at RHIC [15] and LHC [16], rather harder functions are suggested. Within the FONLL approach the Braaten-Cheung-Fleming-Yuan (BCFY) [21] function with $r_c = 0.1$ for charm and the Kartvelishvili [22]

parametrization with $\alpha_b = 29.1$ for bottom are used. In our calculation, to make the shapes of the Peterson functions closer to those from the FONLL approach, the parameters are fixed to $\varepsilon_c = 0.02$ and $\varepsilon_b = 0.001$ (see Fig. 12). In the following numerical predictions of the cross sections for D^0 and $B^{\pm}$ mesons the fragmentation functions are normalized to the branching fractions from Refs. [23–25], i.e. $\mathrm{BR}(c \to D^0) = 0.565$ and $\mathrm{BR}(b \to B^{\pm}) = 0.4$.

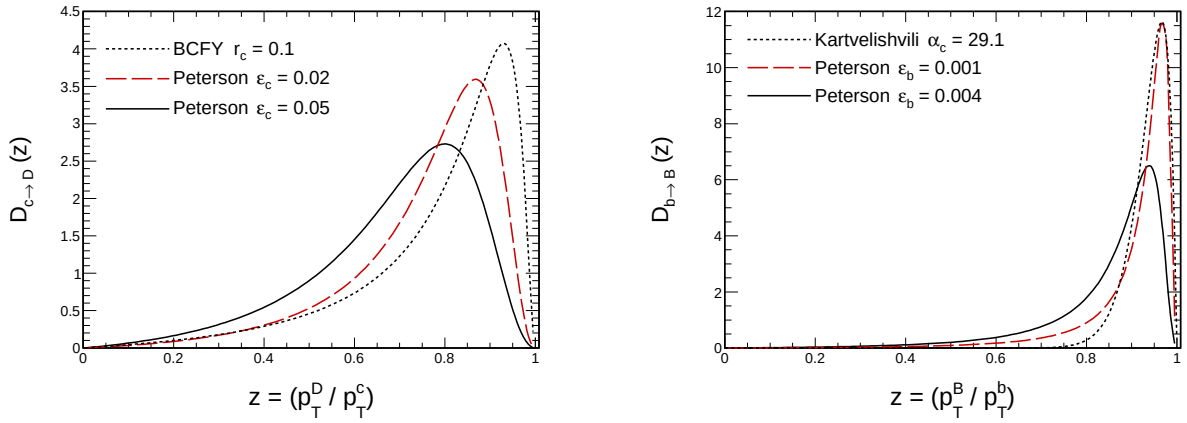

FIG. 12: Different models of the fragmentation functions for charm (left) and bottom (right) quarks. The default functions from the FONLL framework are compared to the Peterson functions with different ε parameters.

D. Cross sections for D^0 and $B^{\pm}$ mesons production

Measurements of charm and bottom cross sections at hadron colliders can be performed in the so-called direct way. This method is based on full reconstruction of all decay products of open charm and bottom mesons, for instance in the $D^0 \to K^-\pi^+$, $D^+ \to K^-\pi^+\pi^+$ or $B^+ \to J/\psi K^+ \to K^+\mu^+\mu^-$ channels. The decay products with an invariant mass from the expected hadron decay combinations, permit direct observation of D or B meson as a peak in invariant mass spectrum. Then, after a substraction of invariant mass continuum the relevant cross section for the meson production can be provided. The same method can be applied for measurement of charm and bottom production rates for the diffractive events.

Numerical predictions of the integrated cross sections for the single- and central-diffractive production of D^0 and $B^{\pm}$ mesons, including relevant experimental acceptance of the ATLAS, LHCb and CMS detectors, are collected in Table I. The kinematical cuts are taken to be identical to those which have been already used in the standard non-diffractive measurements of open charm and bottom production rates at the LHC. The corresponding experimental cross sections for non-diffractive processes are shown for reference. In the case of inclusive production of single D or B meson the ratio of the diffractive integrated cross sections to the non-diffractive one is about $\sim 2\%$ for single- and only about $\sim 0.07\%$ for central-diffractive mechanism. This ratio is only slightly bigger for $D^0\overline{D^0}$ pair production, becoming of about $\sim 3\%$ and 0.1%, respectively. In addition, the relative contribution of the reggeon-exchange mechanisms to the overall diffractive production cross sections is also shown. This relative contribution is about $\sim 24 - 31\%$ for single-diffractive ($\frac{IR}{IP+IR}$) and $\sim 42 - 50\%$ for central-diffractive processes ($\frac{IPIR+IRIP+IRIR}{IPIP+IPIR+IRIP+IRIR}$) for both, charm and bottom flavoured

TABLE I: Integrated cross sections for diffractive production of open charm and bottom mesons in different measurement modes for ATLAS, LHCb and CMS experiments at $\sqrt{s} = 14$ TeV.

Acceptance	Mode	Integrated cross sections, [nb]		
		single-diffractive	central-diffractive	non-diffractive EXP data
ATLAS, $\lvert y\rvert < 2.5$ $p_\perp > 3.5$ GeV	$D^0 + \overline{D^0}$	3555.22 (IR: 25%)	177.35 (IR: 43%)	–
LHCb, $2 < y < 4.5$ $p_\perp < 8$ GeV	$D^0 + \overline{D^0}$	31442.8 (IR: 31%)	2526.7 (IR: 50%)	1488000 ± 182000
CMS, $\lvert y\rvert < 2.4$ $p_\perp > 5$ GeV	$(B^+ + B^-)/2$	349.18 (IR: 24%)	14.24 (IR: 42%)	$28100 \pm 2400 \pm 2000$
LHCb, $2 < y < 4.5$ $p_\perp < 40$ GeV	$B^+ + B^-$	867.62 (IR: 27%)	31.03 (IR: 43%)	$41400 \pm 1500 \pm 3100$
LHCb, $2 < y < 4$ $3 < p_\perp < 12$ GeV	$D^0\overline{D^0}$	179.4 (IR: 28%)	7.67 (IR: 45%)	$6230 \pm 120 \pm 230$

mesons. The ratio does not really change for different measurement modes and different experimental acceptance.

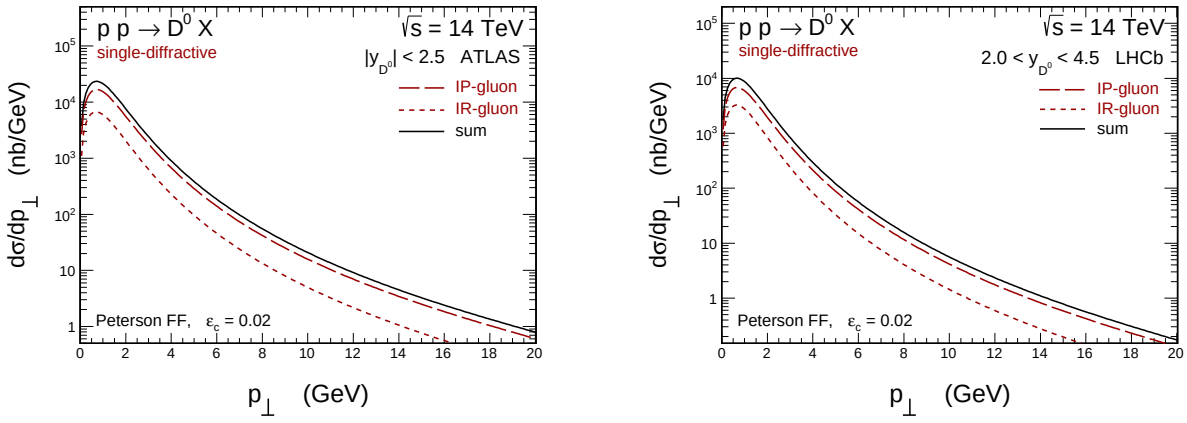

FIG. 13: Transverse momentum distribution of D^0 meson within the ATLAS (left) and the LHCb (right) acceptance for single-diffractive production at $\sqrt{s} = 14$ TeV. Components of the pomeron-gluon (and gluon-pomeron) (long-dashed line) and the reggeon-gluon (and gluon-reggeon) (short-dashed line) contributions are shown separately.

Figures 13 and 14 show transverse momentum distributions of D^0 meson at $\sqrt{s} = 14$ TeV within the ATLAS (left panels) and the LHCb (right panels) acceptance for single- and central-diffractive production, respectively. The contributions of the pomeron- (long-dashed lines) and reggeon-exchange (short-dashed lines) mechanisms are shown separately. These

both contributions have similar shapes of the distributions and differ only in normalization. Therefore, one should not expect a possibility to extract and to test the reggeon component within the special cuts in transverse momentum. The similar distributions (with identical conclusions) but for $B^{\pm}$ meson within the CMS (left panels) and the LHCb (right panels) acceptance are presented in Figs. 15 and 16.

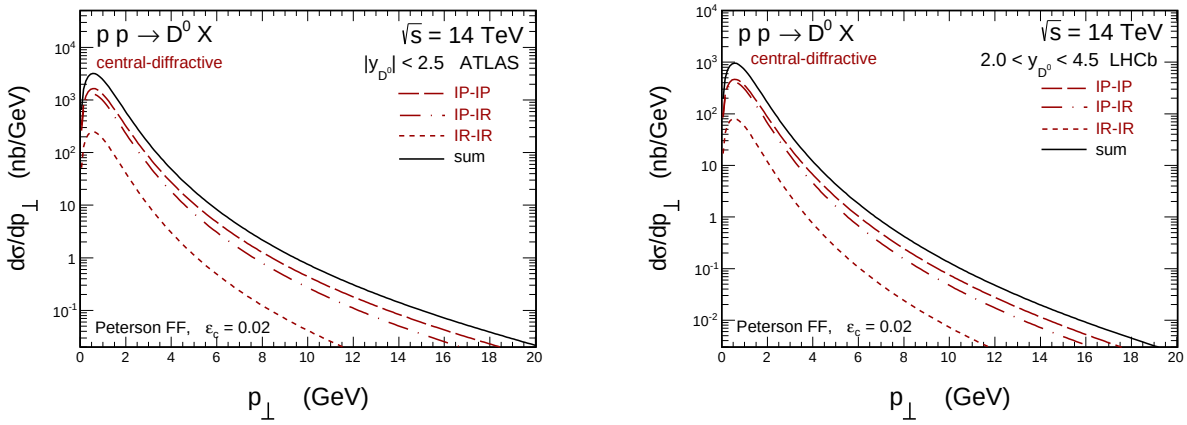

FIG. 14: Transverse momentum distribution of D^0 meson within the ATLAS (left) and the LHCb (right) acceptance for central-diffractive production at $\sqrt{s} = 14$ TeV. Components of the pomeron-pomeron, pomeron-reggeon, reggeon-pomeron and the reggeon-reggeon contributions are shown separately.

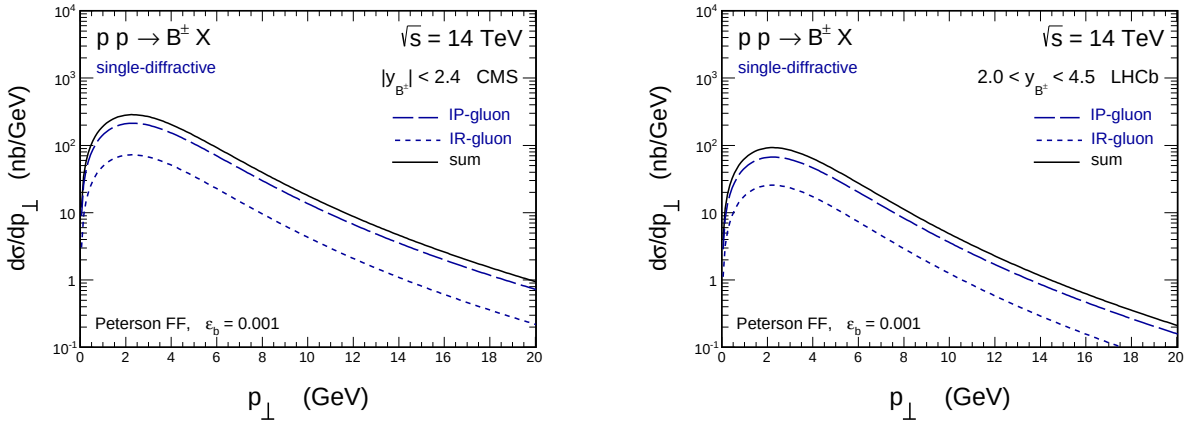

FIG. 15: Transverse momentum distribution of $B^{\pm}$ meson within the CMS (left) and the LHCb (right) acceptance for single-diffractive production at $\sqrt{s} = 14$ TeV. Components of the pomeron-gluon (and gluon-pomeron) (long-dashed line) and the reggeon-gluon (and gluon-reggeon) (short-dashed line) contributions are shown separately.

Figures 17 and 18 show transverse momentum (left panels) and rapidity (right panels) distributions of D^0 (or $\overline{D^0}$) meson at $\sqrt{s} = 14$ TeV within the LHCb acceptance in the case of $D^0\overline{D^0}$ pair production for single- and central-diffractive mechanisms, respectively. The graphical representation of pomeron- and reggeon-exchange contributions is the same as in the previous figures. The rapidity distributions for pomeron-gluon (or reggeon-gluon) and

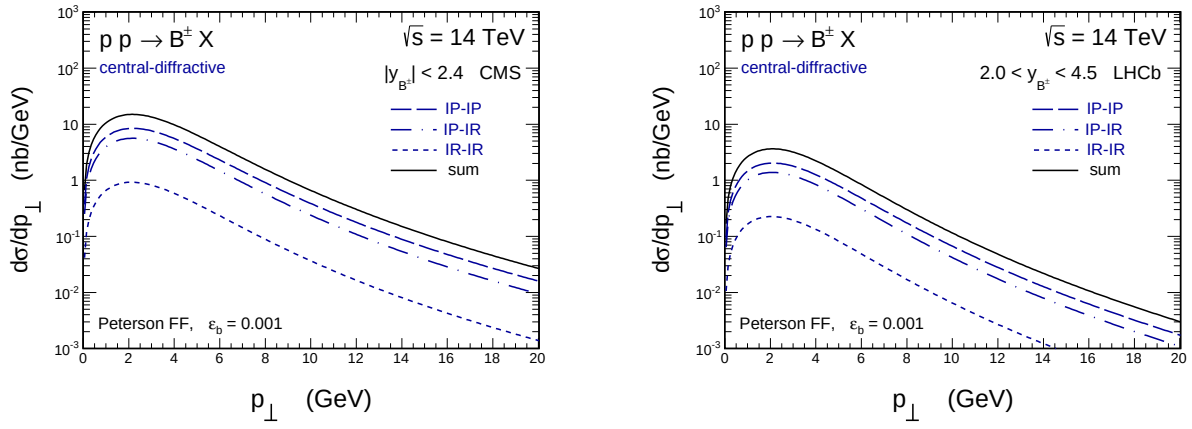

FIG. 16: Transverse momentum distribution of $B^{\pm}$ meson within the CMS (left) and the LHCb (right) acceptance for central-diffractive production at $\sqrt{s} = 14$ TeV. Components of the pomeron-pomeron, pomeron-reggeon, reggeon-pomeron and reggeon-reggeon mechanisms are shown separately.

gluon-pomeron (or gluon-reggeon) mechanisms in the single-diffractive case are shifted to forward and backward rapidities, respectively. Since the rapidity acceptance of the LHCb detector is not symmetric in rapidity and covers only forward region $2 < y_{D^0} < 4$ these both single-diffractive mechanisms contribute to the $D^0\overline{D^0}$ pair diffractive cross section in a quite different way. The situation is shown in more detail in Fig. 19 where the rapidity correlations between D^0 and $\overline{D^0}$ meson are depicted. In all the considered cases these distributions show some correlation along the diagonal. Clearly some shifts of the distributions for the single-diffractive mechanism can be seen, in contrast to the central-diffractive one.

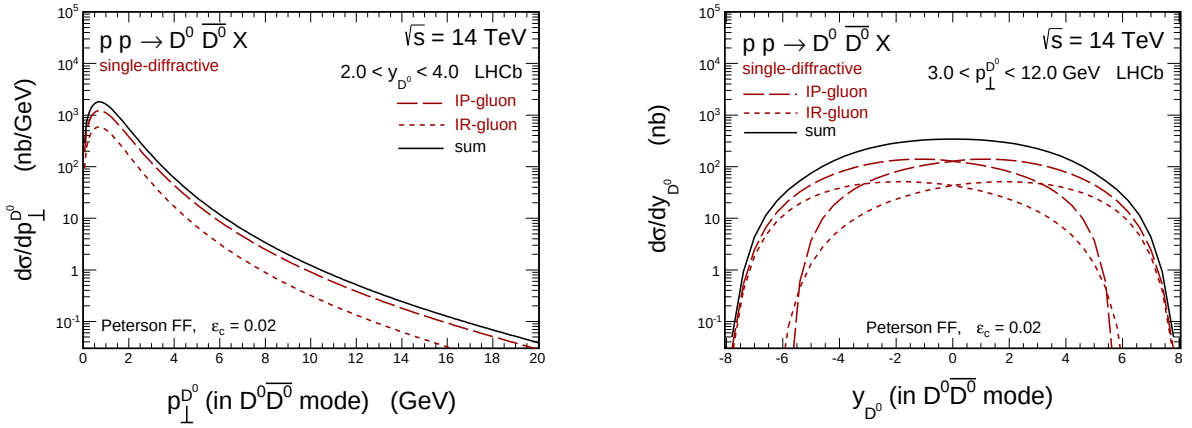

FIG. 17: Transverse momentum (left) and rapidity (right) distributions of D^0 meson within the LHCb acceptance provided that $\overline{D^0}$ was registered too, for the single-diffractive mechanisms at $\sqrt{s} = 14$ TeV. Components of the pomeron-gluon (and gluon-pomeron) (long-dashed line) and the reggeon-gluon (and gluon-reggeon) (short-dashed line) contributions are shown separately.

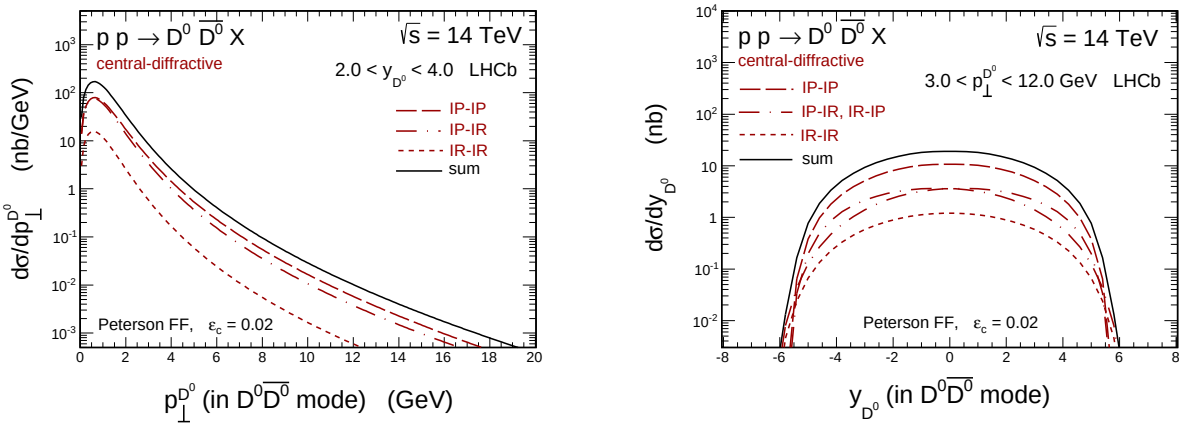

FIG. 18: Transverse momentum (left) and rapidity (right) distributions of D^0 meson within the LHCb acceptance provided that $\overline{D^0}$ was registered too, for the central-diffractive mechanism at $\sqrt{s} = 14$ TeV. Components of the pomeron-pomeron, pomeron-reggeon, reggeon-pomeron and reggeon-reggeon contributions are shown separately.

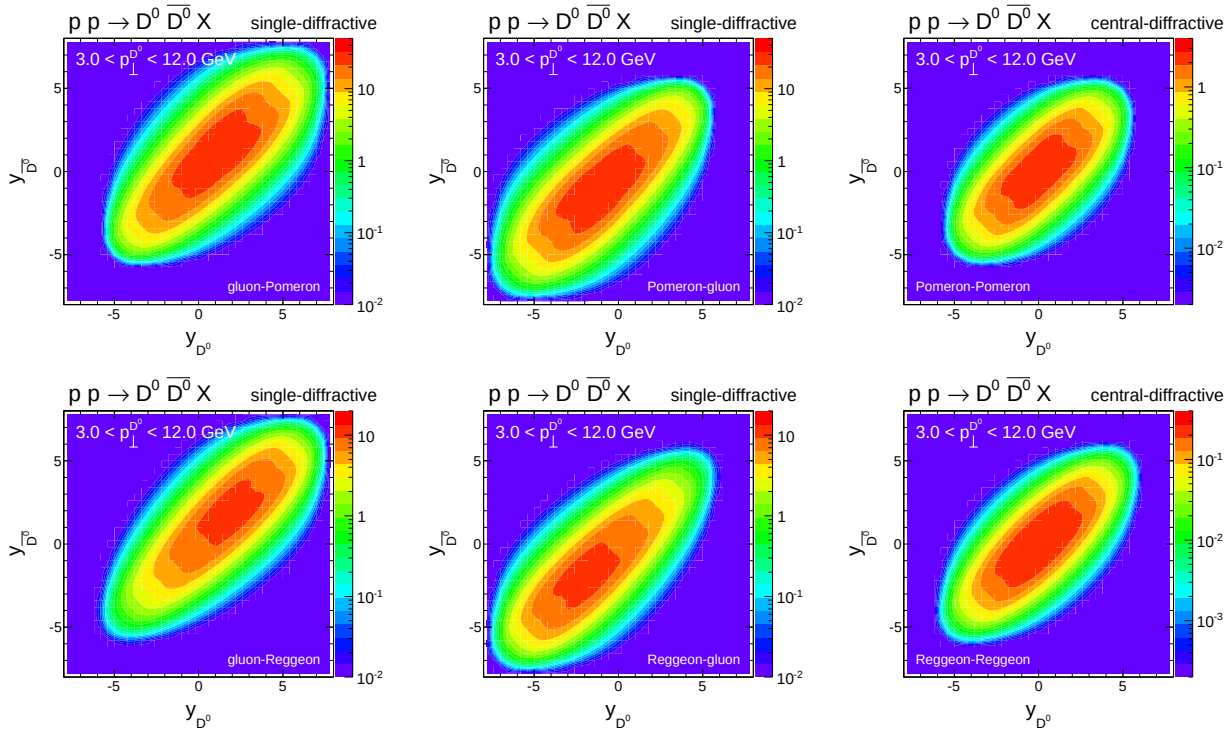

FIG. 19: Double differential cross sections as a function of D^0 and $\overline{D^0}$ rapidities within the LHCb detector acceptance for single- (left and middle panels) and central-diffractive (right panels) production at $\sqrt{s} = 14$ TeV. The top and bottom panels correspond to the pomeron and reggeon exchange mechanisms respectively.

III. CONCLUSIONS

Although there was a lot of theoretical activity in calculating diffractive production of different objects (gauge bosons (W, Z), jets or dijets, Higgs boson, pairs of gauge bosons (W^+W^-) in proton-proton or proton-antiproton collisions, almost no detailed experimental studies were performed and presented in the literature. Such a study would be interesting and important in order to understand mechanism of diffractive production. This is partly so as many reactions considered so far have rather very small cross section. So far there is no common agreement on what is underlying mechanism of diffractive production. Since the underlying dynamics is of nonperturbative nature any detailed studies would be therefore very helpful to shed new light on the problem.

In the present paper we discuss in more detail single- and central- diffractive production of charm and bottom quark-antiquark pairs as well as open charmed and bottom mesons. The corresponding cross sections are rather large.

In the present study we have limited ourselves to the most popular Ingelman-Schlein model of resolved pomeron and reggeon. Although there is no experimental proof for the model and its underlying dynamics it has advantage it was used to describe many diffractive processes at HERA. In the purely hadronic processes considered in the present paper it must be supplemented by including absorption effects due to nonperturbative interaction of hadrons (protons).

In our approach we use diffractive parton distribution in the proton obtained at HERA from the analysis of diffractive structure function of the proton and diffractive production of jets. Both pomeron and reggeon contributions are considered here.

First we have calculated cross sections for $c\bar{c}$ and $b\bar{b}$ production in single and central production. Several quark-level differential distributions are shown and discussed. We have compared pomeron and reggeon contributions for the first time.

In order to make predictions which could be compared with future experimental data in the next step we have included hadronization to charmed (D) and bottom (B) mesons using a practical method of hadronization functions known for other processes. We have shown several inclusive differential distributions for the mesons as well as correlations of D and $\bar{D}$ mesons. In these calculations we have included detector acceptance of the ATLAS, CMS and LHCb collaboration experiments.

The production of charmed mesons is extremely interesting because of the cross section of the order of a few microbarns for ATLAS and CMS and of the order of tens of microbarns for the LHCb acceptance. We have shown that the pomeron contribution is much larger than the subleading reggeon contribution. Especially the LHCb main detector supplemented with VELO (VErtex LOcator) micro-strip silicon detectors installed already in Run I and so-called HERSCHEL (High Rapidity Shower Counters for LHCb) apparatus to be installed in Run II could be used to measure D mesons (main detector) and define rapidity gap nececcesary for diffractive production (VELO and/or HERSCHEL). On the other hand ATLAS and CMS collaboration could use ALFA and TOTEM detectors to measure forward protons. Then different additional differential distributions are possible.

Acknowledgments We are indebted to Guy Wilkinson from the LHCb collaboration for discussion of the LHCb possibilities and Wolfgang Schäfer for several interesting discussions of diffractive processes and heavy quark production in particular. We wish to thank Rafał

Staszewski and Maciej Trzebiński for continues interest in our studies. This work was partially supported by the Polish NCN grant DEC-2013/09/D/ST2/03724.

---

[1] G. Ingelman, P.E. Schlein, Phys. Lett. B152 256 (1985).
[2] M. Klasen, G. Kramer, Phys. Rev. **D80** (2009) 074006.
[3] L. Alvero, J.C. Collins, J. Terron and J.J. Whitmore, Phys. Rev. **D59** (1999) 074022.
[4] A. Cisek, W. Schäfer and A. Szczurek, Phys. Rev. **D80** (2009) 074013.
[5] M. Łuszczak, A. Szczurek and Ch. Royon, arXiv:1409.1803 [hep-ph].
[6] M. Łuszczak, R. Maciuła and A. Szczurek, Phys. Rev. **D84** (2011) 114018.
[7] C. Marquet, C. Royon, M. Trzebiński and R. Zlebcik, Phys. Rev. **D87** (2013) 034010.
[8] R. Maciula and A. Szczurek, Phys. Rev. D **87**, 094022 (2013) [arXiv:1301.3033 [hep-ph]].
[9] A. Aktas *et al.* [H1 Collaboration], Eur. Phys. J. C **48** (2006) 715.
[10] A.D. Martin, W.J. Stirling, R.S. Thorne and G. Watt, Eur. Phys. J. C **63** (2009) 653.
[11] V.A. Khoze, A.D. Martin and M.G. Ryskin, Eur. Phys. J. **C18**, 167 (2000).
[12] U. Maor, AIP Conf. Proc. **1105**, 248 (2009).
[13] B. Andersson, G. Gustafson, G. Ingelman and T. Sjostrand, Phys. Rept. **97**, 31 (1983).
[14] B. R. Webber, Nucl. Phys. B **238**, 492 (1984).
[15] M. Cacciari, P. Nason and R. Vogt, Phys. Rev. Lett. **95**, 122001 (2005) [hep-ph/0502203].
[16] M. Cacciari, S. Frixione, N. Houdeau, M. L. Mangano, P. Nason and G. Ridolfi, J. High Energy Phys. **10**, 137 (2012) [arXiv:1205.6344 [hep-ph]].
[17] C. Peterson, D. Schlatter, I. Schmitt and P. M. Zerwas, Phys. Rev. D **27**, 105 (1983).
[18] F. D. Aaron *et al.* [H1 Collaboration], Eur. Phys. J. C **59**, 589 (2009) [arXiv:0808.1003 [hep-ex]].
[19] A. Heister *et al.* [ALEPH Collaboration], Phys. Lett. B **512**, 30 (2001) [hep-ex/0106051].
[20] G. Abbiendi *et al.* [OPAL Collaboration], Eur. Phys. J. C **29**, 463 (2003) [hep-ex/0210031].
[21] E. Braaten, K. -m. Cheung, S. Fleming and T. C. Yuan, Phys. Rev. D **51**, 4819 (1995) [hep-ph/9409316].
[22] V. G. Kartvelishvili, A. K. Likhoded and V. A. Petrov, Phys. Lett. B **78**, 615 (1978).
[23] E. Lohrmann, arXiv:1112.3757 [hep-ex].
[24] J. Beringer *et al.* [Particle Data Group Collaboration], Phys. Rev. D **86**, 010001 (2012).
[25] T. Aaltonen *et al.* [CDF Collaboration], Phys. Rev. D **77**, 072003 (2008) [arXiv:0801.4375 [hep-ex]].